HYDROLOGICAL PROCESSES, VOL. 10, 1619–1628 (1996)

SNOW WETNESS ESTIMATES OF VEGETATED TERRAIN FROM SATELLITE PASSIVE MICROWAVE DATA

CHANGYI SUN

Forest Resources, Utah State University, Logan, UT 84322-5215, USA

CHRISTOPHER M. U. NEALE

Biological and Irrigation Engineering, Utah State University, Logan, UT 84322-4105, USA

AND

JEFFREY J. McDONNELL

College of Environmental Science and Forestry, SUNY, Syracuse, NY 13210-2779, USA

ABSTRACT

The Special Sensor Microwave/Imager (SSM/I) radiometer is a useful tool for monitoring snow wetness on a large scale because water content has a significant effect on the microwave emissions at the snowpack surface. To date, SSM/I snow wetness algorithms, based on statistical regression analysis, have been developed only for specific regions. Inadequate ground-based snow wetness measurements and the non-linearity between SSM/I brightness temperatures (T_Bs) and snow wetness over varied vegetation covered terrain has impeded the development of a general model. In this study, we used a previously developed linear relationship between snowpack surface wetness (% by volume) and concurrent air temperature (°C) to estimate the snow wetness at ground weather stations. The snow condition (snow free, dry, wet or refrozen snow) of each SSM/I pixel (a 37 × 29 km area at 37·0 GHz) was determined from ground-measured weather data and the T_B signature. SSM/I T_Bs of wet snow were then linked with the snow wetness estimates as an input/output relationship. A single-hidden-layer back-propagation (backprop) artificial neural network (ANN) was designed to learn the relationships. After training, the snow wetness values estimated by the ANN were compared with those derived by regression models. Results show that the ANN performed better than the existing regression models in estimating snow wetness from SSM/I data over terrain with different amounts of vegetation cover.

KEY WORDS SSM/I radiometer; snow wetness; passive microwave; vegetated terrain

INTRODUCTION

The Special Sensor Microwave/Imager (SSM/I) radiometers, on board the Defense Meteorological Satellite Program (DMSP) F8, F10 and F11 satellites, have been used to produce global hydrological data (Ferraro *et al.*, 1994). The SSM/I is a seven-channel, four-frequency, linearly polarized, passive microwave radiometric system (Hollinger, 1989), which measures both vertically (V) and horizontally (H) polarized brightness temperatures (T_Bs), at 19·35, 37·0 and 85·5 GHz, and vertically polarized temperatures at 22·235 GHz. Unlike *in situ* methods, the SSM/I provides an indirect estimate of snow parameters by using parameter retrieval algorithms, with T_B values as inputs. To develop the algorithm, SSM/I T_B observations along with ground truth data are required.

Because of the limited penetration depth of the passive microwave signal, the SSM/I registers wet snow when the surface layer contains water even if the bulk of the snowpack is dry (Ulaby *et al.*, 1986). The water between the snow grains causes a significant increase in internal absorption of the microwave radiation thereby increasing the snow emissivity (Rango *et al.*, 1979). Foster *et al.* (1984) indicated that T_B for frequencies above 10 GHz increases rapidly with increasing snow wetness (i.e. the liquid water content)

CCC 0885–6087/96/121619-10

up to 4% by volume, and decreases gradually with snow wetness above 5% by volume. It is therefore possible to monitor large-scale snow wetness at the snowpack surface using the SSM/I radiometer.

Nevertheless, the development of an SSM/I snow wetness algorithm has been impeded by the lack of adequate ground-based snow wetness measurements. In a field experiment, Sun *et al.* (1995) used a dielectric probe to sample snow wetness at the snowpack surface (top 10 cm layer) over forested, mountainous and non-vegetated flat areas. They found that snow wetness, W_{SNOW} (% by volume), was related ($R^2 = 0{\cdot}708$) to concurrent air temperature, T_{AIR}(°C), as

$$W_{SNOW} = 1{\cdot}0285 + 0{\cdot}5708 T_{AIR} \quad (1)$$

Based upon this regression model, they estimated the snow wetness concurrently with T_B observations for a flat, sparsely vegetated SSM/I pixel and derived a regression-based ($R^2 = 0{\cdot}950$) SSM/I snow wetness algorithm in terms of T_B difference, T_D (K), as

$$W_{SNOW} = -4{\cdot}75 + 339{\cdot}53 T_D^{-1} - 6159{\cdot}53 T_D^{-2} + 40112{\cdot}00 T_D^{-3} \quad (2)$$

where T_D = T19V − T37H. However, they found that the algorithm was not applicable in areas dominated by evergreen forest. The overlying vegetation depolarized the signal. This decreased the temperature difference T_D (Hall *et al.*, 1991) and resulted in an overestimate of snow wetness.

Because of the complexity between T_B and snow wetness over varied terrain and vegetation cover, a non-linear retrieval method is needed to obtain snow wetness values from microwave data. Artificial neural networks (ANNs) are non-linear models that have been used to retrieve snow parameters from passive microwave data (Tsang *et al.*, 1992; Davis *et al.*, 1993). ANNs can learn T_B patterns whose complexity and non-linearity make it impossible to use regression approaches. According to Simpson (1992), the back-propagation (backprop) ANN method is identical to the stochastic approximation technique for finding a relationship between inputs and outputs when the inputs and outputs are extremely noisy.

To develop a more widely applicable snow wetness algorithm, we used Equation (1) and air temperature data to estimate snow wetness over a variety of geographical areas. We tested the input/output relationships between SSM/I T_B observations and our snow wetness estimates, and designed a backprop ANN to retrieve snow wetness from SSM/I data.

STUDY SITE AND DATA

The study area (located in the western United States and bounded by latitude of 40°N to 45°N and longitude of 100°W to 115°W, Figure 1) was selected as it contained both plains and mountainous regions and diverse vegetation cover. SSM/I T_B values and ground-based climate data from 1 October 1989 to 30 May 1990 in the area were used for the study.

SSM/I T_B values from the DMSP-F8 satellite were obtained from the Naval Research Laboratory. Both SSM/I 85·5 GHz channels failed on DMSP-F8, so only T_B values of the lower frequency channels, T19V, T19H, T22V, T37V and T37H, were available.

Ground-based measurements of daily snow water equivalent (SWE), and maximum, minimum and average air temperature were obtained for mountainous terrain from the Soil Conservation Service (SCS) SNOwpack TELemetry (SNOTEL) system. Data for daily snow depth (SD), maximum and minimum air temperature and air temperature at the satellite overpass time were obtained for the plains from the National Oceanic and Atmospheric Administration (NOAA) cooperative weather observation network.

GROUND-BASED SNOW CLASSIFICATION

Daily snow conditions at each SNOTEL or NOAA weather station at either 0600 or 1800 (the DMSP-F8 local crossing time) were classified as: (i) snow free if SWE or SD was equal to zero; (ii) dry snow if SWE or

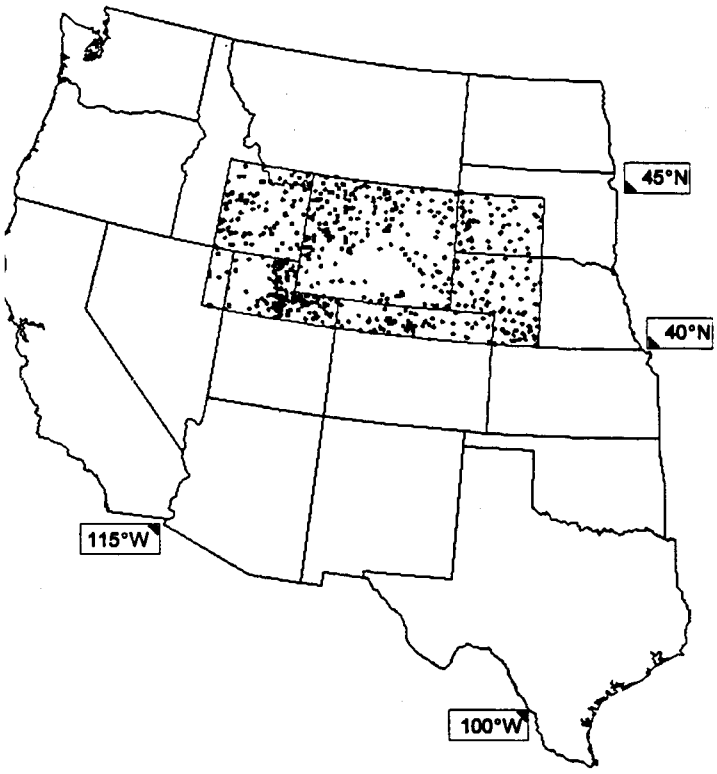

Figure 1. The study area and the ground-based weather stations

SD increased from the previous observation time and the concurrent air temperature was below 3·5°C; (iii) wet snow if SWE or SD was not equal to zero and the concurrent air temperature was greater than or equal to 3·5°C; or (iv) refrozen snow if the concurrent air temperature was below freezing and the snow condition of the previous overpass was either wet or refrozen. We used 3·5°C as the cut-off point to avoid adding dry snow pixels to the wet snow data set in areas having spatially variable air temperatures. As can be seen from Equation (1), air temperatures greater than 3·5°C can be interpreted as wet snow ($W_{SNOW} > 3\%$ by volume, International Commission on Snow and Ice Classification System).

For the SNOTEL stations, air temperatures at 0600 and 1800 (the SSM/I overpass times) were used as the daily minimum and average air temperature, respectively. For the NOAA weather stations, a temperature measurement recorded between 0400 and 0700 was used to calculate snow wetness for the 0600 flyby data, and a temperature measured between 1600 and 1900 was used with the image acquired at 1800. If air temperatures were not recorded during these intervals, the air temperature at 0600 was equal to the minimum air temperature and that at 1800 was interpolated as follows. The maximum air temperature was assumed to occur at 1400 and was linearly decreased to the temperature at observing time if after 1400, or the maximum air temperature of the previous day was decreased to the air temperature at observing time if before 1400.

INTEGRATION OF SSM/I AND SNOW WETNESS DATA

Since the latitude/longitude coordinates of the SSM/I pixels change with each overpass, a neighbourhood merging method (Sun, 1996) was employed to integrate the SSM/I and snow wetness data into one database. This was done by searching for ground weather stations within a 15-km radius of the SSM/I latitude/longitude location (i.e. approximately the size of a 37·0 GHz pixel) and averaging the air temperature in each SSM/I pixel. Snow wetness at each pixel was then estimated using Equation (1).

ANN-BASED SNOW CLASSIFICATION

Because of the temporal variability of air temperature, errors in the classification of snow wetness could result in different snow conditions being related to SSM/I pixels of similar T_B patterns. To minimize classification errors, the SSM/I ANN snow classifier (Sun, 1996) was also used to classify snow conditions in the database. Only data of those SSM/I pixels classified as wet snow by both ground-based and ANN-based classification methods were used as the input/output data pairs (i.e. input of five SSM/I T_B values and one desired output of snow wetness). Thus, a subset database of input/output data pairs was created.

ANN TOPOLOGY AND LEARNING ALGORITHM

A single-hidden-layer backprop ANN, as illustrated in Figure 2, was created. The ANN consists of a series of three layers: one input layer, one hidden layer and one output layer. Each layer has a number of nodes: five input nodes for the input of five T_B values, one output node for the mapping output that estimates the desired output of snow wetness and a set of hidden nodes for internal representation of the mapping between the input and output nodes. Nodes of adjacent layers are fully connected. Each connection is initially assigned a small random value (connection weight) between −0·1 and 0·1. Given the number of nodes in each layer from input to output as a sequence, the ANN topology is represented as 5-N-1, where N is the number of hidden nodes that was selected, either 2, 5, 10 or 20. In addition, a bias node, functioning similarly to a constant in a regression, is connected to the nodes in the hidden and output layers.

The error back-propagation training algorithm (Zurada, 1992) was applied to train the ANNs. This method allows inputs to flow forwards through the hidden layer to the output layer. The inputs are used to calculate the node outputs in each hidden and output layer. Each node in the hidden layer and output layer decides its output by calculating the *net*, which is the sum of all of its incoming connection weights, W, multiplied by the node outputs, X, from the previous layer:

$$net_i^{(S)} = \sum_{ij} X_i^{(S-1)} W_{ij} \tag{3}$$

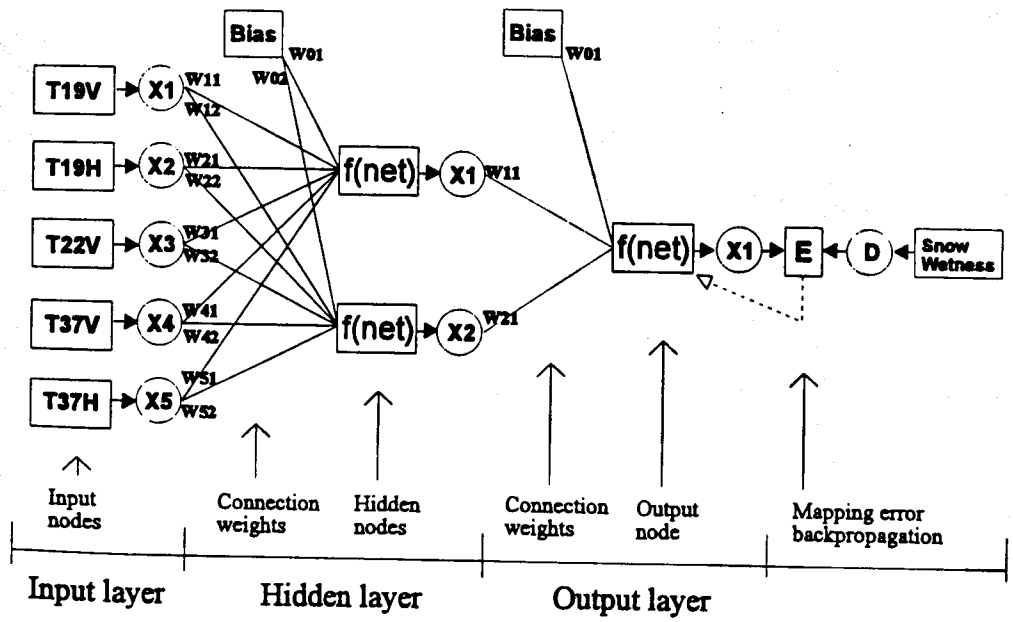

Figure 2. Example of a 5-2-1 ANN using backprop training

where S denotes the state of current layer. Then, the *net* is transferred by the activation function, which gives an output between 0 and 1:

$$X_i^{(S)} = f(net_i^{(S)}) = 1/(1 + \exp(-net_i^{(S)})) \tag{4}$$

After calculating node output in the output layer, the mapping error, E, between desired output, D, and node output, X, is measured:

$$E_i^{(S)} = \tfrac{1}{2}(D_i^{(S)} - X_i^{(S)})^2 = \tfrac{1}{2}(D_i^{(S)} - f(net_i^{(S)}))^2 \tag{5}$$

The error is then propagated backwards from the output layer to the input layer. The connections weights are adjusted to minimize the error, so that the calculated output is more like the desired output. In back-propagation, the error is used in obtaining the error gradient, ∇E:

$$\nabla E_i^{(S)} = -(\partial E_i^{(S)}/\partial X_i^{(S)})(\partial X_i^{(S)}/\partial W_{ij}) = -(D_i^{(S)} - X_i^{(S)})f'(net_i^{(S)})X_i^{(S-1)} \tag{6}$$

Because there is no desired node output in the hidden layer, the mapping error of each node in this layer is derived by a weighted sum of error gradients from the output layer:

$$E_i^{(S)} = \sum_{ij} W_{ij}^{(S+1)} \nabla E_i^{(S+1)} \tag{7}$$

and the error gradient is:

$$\nabla E_i^{(S)} = -E_i^{(S)} f'(net_i^{(S)}) X_i^{(S-1)} \tag{8}$$

The error gradients in each layer are propagated back to adjust the connection weight by:

$$W_{ij}^{(t)} = W_{ij}^{(t-1)} - \eta \nabla E_i^{(S)} + \alpha \Delta W_{ij}^{(t-1)} \tag{9}$$

where t is the time when the weight is updated, η is the learning rate and α is the momentum term (Rumelhart *et al.*, 1986). In this study, the learning rate was determined at 0·05, 0·10 and 2·0 for each ANN topology. The momentum term was set at 0·09.

ANN TRAINING, VALIDATION AND TESTING

As indicated by Masters (1993), the proportional representation of classes in the training data set can have a profound influence on the ANN performance. The frequency distributions of data elements may also be important to the ANN training (Sun *et al.*, 1996). Consequently, data elements in the subset database were divided into groups according to the frequency distributions of snow wetness. Based on the smallest data elements in the groups (Table I), six data elements of each snow wetness group were randomly selected to form the training data set. The rationale was to make the data sets as representative of the whole data and as balanced in size for each group as possible. From the remaining elements, a validation data set was also randomly created.

The activation function [Equation (4)] applied to the net input of nodes in the hidden and output layers maps the net output into the range between 0 and 1 (Zurada, 1992). Accordingly, the T_B inputs were scaled between 0 and 1 with respect to a range from 200 to 270 K to represent the input attributes in the ANN. The output, between 0 and 1, for snow wetness represents a water content of 0 to 10% by volume.

The training process was started by running the ANN, which involved forward feeding node outputs by Equations (3) and (4) from the input to output layer, backward propagating mapping errors from the

Table I. Input/output data pairs selected for ANN training and validation

Snow wetness (% by volume)	Number of input/output data pairs		
	Entire data set	Training data set	Validation data set
0–1	50	6	4
1–2	25	6	4
2–3	24	6	4
3–4	18	6	4
4–5	14	6	4
5–7	8	6	2
7–10	9	6	2
Total	148	42	24

output to input layer to adjust the connection weights by Equations (5)–(9) and calculating the root-mean-squared (RMS) error after all the input/output pairs in the training data set were processed. The RMS error was computed on the validation data set by:

$$RMS = \sqrt{\frac{1}{nq} \sum_{n} \sum_{q} (D_i - X_i)^2} \tag{10}$$

where n is the number of input/output data pairs in the data set and q is the number of nodes in the output layer. The training run was repeated until a minimum RMS error was reached.

We evaluated the performances of the ANNs using SSM/I T_B data obtained in 1990 over flat, sparsely vegetated terrain by the DMSP-F11 satellite combined with air temperature-derived [Equation (1)] snow wetness estimates (Sun *et al.*, 1995). After each training, the correlation coefficient, r, between the ANN-retrieved and air temperature-derived values was examined. The ANN with the overall largest r value was used for the follow-up comparisons.

In addition to Equation (2), we developed a multiple regression model to describe the relationship of snow wetness to T19V, T19H, T22V, T37V and T37H based on the training data sampled over a varied vegetation covered region. Comparison between snow wetness values obtained using the ANN model, the regression models and the air temperature model [Equation (1)] were made using statistical inference in terms of r and t test (SAS Institute Inc., 1988).

RESULTS AND DISCUSSION

Table II summarizes the training and testing performance of each ANN topology at different learning rates. There was no evidence that a slower or a higher learning rate improves the ANN performance (i.e. a smaller minimum RMS error). The relatively higher minimum RMS error in each ANN topology at a learning rate of 0·05 could be a sign that the ANN became stuck in a local minimum of the error function [Equation (10)] when adjusting the connection weights (Zurada, 1992). It might also be that these ANNs had many equally good global minima (Masters, 1993) as the RMS errors were similar. Consequently, the best ANN (i.e. the 5-2-1 ANN trained at a learning rate of 0·10 ANN with r of 0·542 in testing) was derived from a number of training runs at different learning rates by trial and error.

From a statistical point of view, the relationship between snow wetness, W_{SNOW}, and all five T_B values in the training data was defined by the multiple regression model ($R^2 = 0{\cdot}362$):

$$W_{SNOW} = -114{\cdot}49 + 0{\cdot}4(T37V) + 0{\cdot}56(T37H) - 0{\cdot}64(T22V) + 0{\cdot}4(T19V) - 0{\cdot}26(T19H) \tag{11}$$

Only about 26% ($r = 0{\cdot}511$) of the variation in snow wetness was explained by Equation (11) in the validation data set (Table III). The weak linear relationship could result from the complexity between T_B and

Table II. Summary of the ANNs training and testing performances

ANN		Training results		Testing results
Topology	Learning rate	Total runs	Minimum RMS	r
5-2-1	0·05	1149	0·22398	0·539
	0·10	558	0·22119	0·542
	0·20	320	0·22250	0·533
5-5-1	0·05	1125	0·22519	0·536
	0·10	581	0·22174	0·539
	0·20	309	0·22241	0·528
5-10-1	0·05	1104	0·22536	0·525
	0·10	597	0·22252	0·528
	0·20	315	0·22237	0·516
5-20-1	0·05	997	0·22551	0·515
	0·10	566	0·22280	0·509
	0·20	337	0·22257	0·495

snow wetness over varied vegetation covered terrain. This was confirmed by finding that snow wetness estimates obtained using Equation (11) were highly correlated ($r = 0{\cdot}859$) but significantly different ($p < 0{\cdot}05$) than the air temperature-based values in the test data set [see Equation (11) vs. Equation (1) in Table III], which were sampled at a sparsely vegetated location. The high correlation suggests that the regression model [Equation (11)] learned the general trend between snow wetness and T_B values, whereas the significant difference in group means suggests that the amount of overlying vegetation influenced the microwave emission behaviour, causing an underestimation by Equation (11) in sparsely vegetated areas (Figure 3) and an overestimation by Equation (2) over a varied vegetation covered region (Figure 4).

However, both significant correlation and equal variance were found between ANN-retrieved and air temperature-based snow wetness in the test data set [see ANN vs. Equation (1) in Table III]. These statistics indicate that the ANN not only learned the general relationship between snow wetness and T_B values, but also accounted for the depolarization effect of vegetation on microwave emission. Such evidence was also seen in model comparison (Table IV), for only ANN snow wetness estimates were highly correlated and similar to those obtained by the regression model on the data set from which the regression model was developed.

Although the ANN approach was comparable with, and more robust than, the regression method (Table IV), significant differences were found between ANN-retrieved and air temperature-based snow wetness in the validation data set, for the associated p value is 0·009 in paired comparisons (Table III). As seen in Figure 4, most of the uncertainties were related to medium vegetated areas having air temperature-derived snow wetness values below 3% or above 6% by volume. That SSM/I T_B signatures of medium vegetated

Table III. Comparison of model-retrieved versus air temperature-derived (GRND) snow wetness

Model vs. GRND	Validation data set			Test data set		
	r	t Test* ($p > \|t\|$)		r	t Test* ($p > \|t\|$)	
		Group means	Paired comparisons		Group means	Paired comparisons
ANN vs. Eq. (1)	0·585	0·046	0·009	0·862	0·617	0·384
Eq. (2) vs. Eq. (1)	0·194	0·000	0·000	0·975	0·993	0·952
Eq. (11) vs. Eq. (1)	0·511	0·063	0·014	0·859	0·010	0·009

* Group means: testing whether the variance of the two group are the same
Paired comparisons: testing whether the mean difference between the paired variables is different from zero

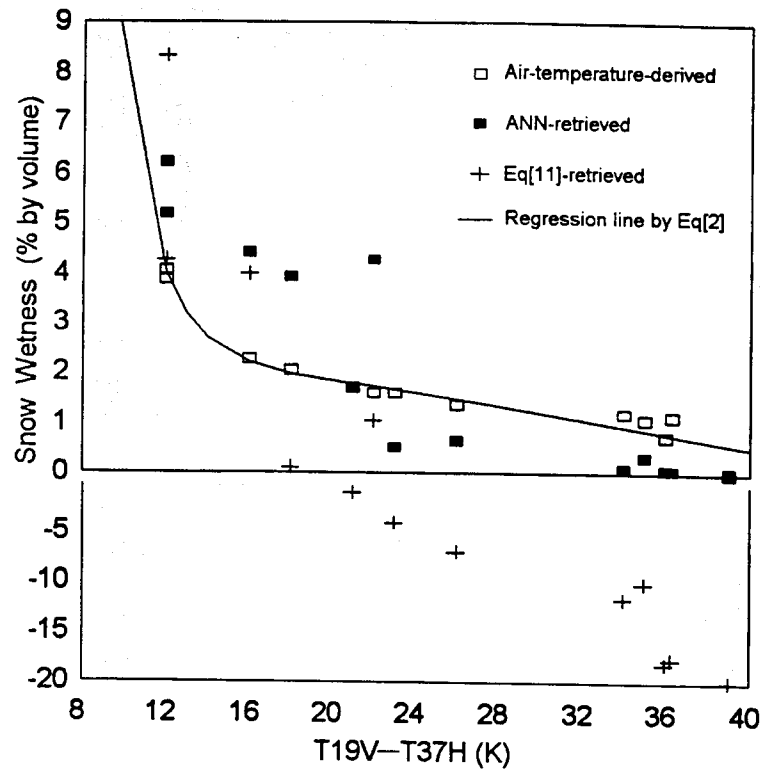

Figure 3. Comparison between model-retrieved and air temperature-derived snow wetness in the test data set

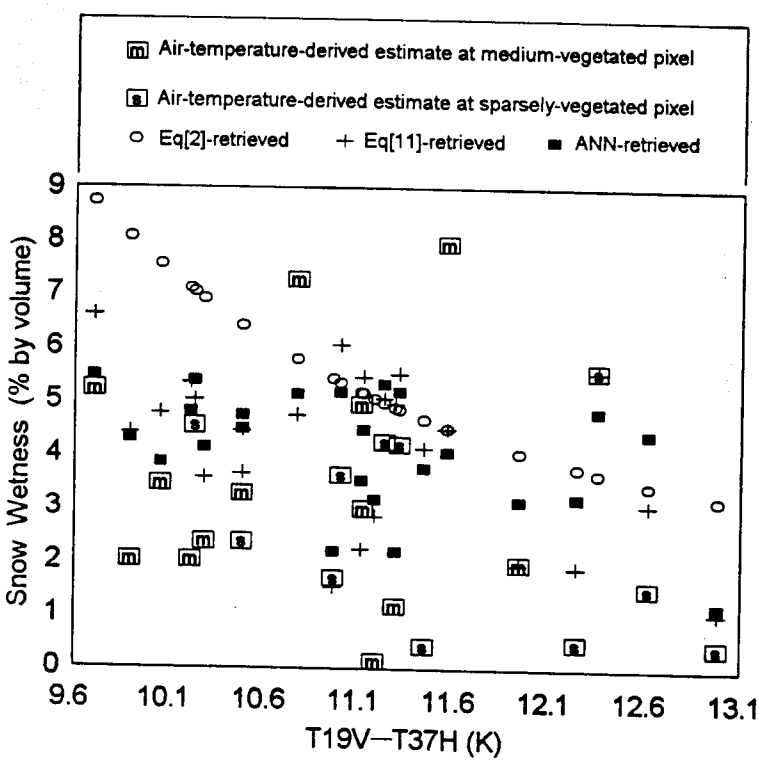

Figure 4. Comparison between model-retrieved and air temperature-derived snow wetness in the validation data set

Table IV. Comparison between model-retrieved snow wetness

Model vs. Model	Validation data set			Test data set		
	r	t Test* ($p > \|t\|$)		r	t Test* ($p > \|t\|$)	
		Group means	Paired comparisons		Group means	Paired comparisons
ANN vs. Eq. (2)	0·444	0·001	0·000	0·892	0·619	0·380
ANN vs. Eq. (11)	0·769	0·973	0·948	0·887	0·009	0·003
Eq. (2) vs. Eq. (11)	0·445	0·002	0·000	0·863	0·010	0·009

* Group means: testing whether the variance of the two group are the same
Paired comparisons: testing whether the mean difference between the paired variables is different from zero

areas with low snow wetness are similar to those of sparsely vegetated areas with high snow wetness, may be a result of: (i) the lack of input/output data patterns in a high snow wetness range (Table I), resulting in the selection of a smaller training data set in which certain significant input/output relations were lost by random selection; and (ii) uncertainties in estimating snow wetness using Equation (1), owing to the temporal and spatial variability of air temperature over different geographical areas.

CONCLUSIONS

This study has used a backprop ANN to find a relationship between SSM/I T_B observations of an area and snow wetness derived from air temperature data. Results show that the ANN may overcome the limitations of the existing regression models in estimating snow wetness from SSM/I data over varied terrain with varying vegetation cover.

Although the ANN can learn input/output relationships from noisy data, a sufficient number of representative input/output data can improve the ANN performance. As more representative input/output relationships are established by using data from varied vegetation covered terrain, we expect our ability to predict snow wetness to improve.

ACKNOWLEDGEMENT

This study was supported by the NASA WetNet Project (Contract NAG8-897).

REFERENCES

Davis, D. T., Chen, Z., Tsang, L., Hwang, J. and Chang, A. T. C. 1993. 'Retrieval of snow parameters by iterative inversion of a neural network', *IEEE Trans. Geosci. Rem. Sens.*, **31**(4), 842–852.

Ferraro, R., Grody, N., Forsyth, D., Garey, R., Basist, A., Janowiak, J., Weng, F., Marks, G.F. and Yanamandra, R. 1994. 'Microwave measurements produce global climatic, hydrologic data', *Eos Trans., AGU*, **75**(30), July 26.

Foster, J.L., Hall, D. K., Chang, A. T. C., and Rango, A. 1984. 'An overview of passive microwave snow research and results', *Rev. Geophys. Space Phys.*, **22**(2), 195–208.

Hall, D. K., Sturm, M., Benson, C. S., Chang, A. T. C., Foster, J. L., Garbeil, H. and Chacho, E. 1991. 'Passive microwave remote and in situ measurements of Arctic and Subarctic snow cover in Alaska', *Remote Sens. Environ.*, **38**, 161–172.

Hollinger, J. P. 1989. *DMSP Special Sensor Microwave/Imager calibration/validation, Final Report*, Vol. I. Naval Research Laboratory, Washington, D.C., USA.

Masters, T. 1993. *Practical Neural Network Recipes in C++*. Academic Press Inc., San Diego, CA, USA.

Rango, A. 1993. 'II. Snow hydrology processes and remote sensing', *Hydrol. Process.* **7**, 121–138.

Rango, A., Chang, A. T. C., and Foster, J. L. 1979. 'The utilization of spaceborne microwave radiometers for monitoring snowpack properties', *Nord. Hydrol.*, **10**, 25–40.

Rumelhart, D. E., Hinton, G. E. and Williams, R. J. 1986. 'Learning internal representations by error propagation', in Rumelhart, D. E., McClelland, J. L., and the PDP Research Group (Eds), *Parallel Distributed Processing: Explorations in the Microstructure of Cognition*. Vol. 1: *Foundations*. MIT Press, Cambridge, MA, USA. pp. 318–362.

SAS Institute Inc. 1988. *SAS/STAT® User's Guide, Release 6.03 Edition*. SAS Institute Inc., Cary, NC, USA.

Simpson, P. K. 1992. 'Foundations of neural networks', in Sanchez-Sinencio, E. and Lau, C. (Eds), *Artificial Neural Networks: Paradigms, Applications, and Hardware Implementations*. IEEE PRESS, Piscataway, NJ, USA. pp. 3–24.

Sun, C. 1996, 'A neural network approach to SSM/I land surface snow classification', in *Integration of SSM/I and In Situ Data for Snow Studies from Space*, chap. 3, Ph.D. Thesis, Utah State University, Logan, UT, USA.

Sun, C., Neale, C. M. U. and McDonnell, J. J. 1995. 'Relationship between snow wetness and air temperature and its use in the development of an SSM/I snow wetness algorithm', in *Proc. AGU 15th Ann. Hydrology Days*, pp. 271–180.

Sun, C., Neale, C. M. U. and McDonnell, J. J. 1996. 'The potential of using artificial neural network in estimation of snow water equivalent from SSM/I data', in *Proc. AGU 16th Annual Hydrology Days*, pp. 499–509.

Tsang, L., Chen, Z., Oh, S., Marks II, R. H. and Chang, A. T. C., 1992. 'Inversion of snow parameters from passive microwave remote sensing measurements by a neural network trained with a multiple scattering model', *IEEE Trans. Geosci. Rem. Sens.*, **30**(5), 1015–1024.

Ulaby, F. T., Moore, R. K. and Fung, A. K. 1986. *Microwave Remote Sensing: Active and Passive*, Vol. III, *From Theory to Applications*. Artech House, Dedham, MA, USA.

Zurada, J. M. 1992. *Introduction to Artificial Neural Systems*. West Publishing Co., St. Paul, MN, USA.